Carbohydrate Polymers 98 (2013) 1326–1334

Contents lists available at ScienceDirect

Carbohydrate Polymers

journal homepage: www.elsevier.com/locate/carbpol

Carboxymethyl chitosan-poly(amidoamine) dendrimer core–shell nanoparticles for intracellular lysozyme delivery

Xiaoyang Zhang[a], Jun Zhao[a], Yan Wen[b], Chuanshun Zhu[a], Jun Yang[c], Fanglian Yao[a,*]

[a] School of Chemical Engineering and Technology, Key Laboratory of Systems Bioengineering of Ministry of Education, Tianjin University, Tianjin 300072, China
[b] School of Science, Tianjin University of Commerce, Tianjin 300134, China
[c] Key Laboratory of Bioactive Materials, Ministry of Education, College of Life Sciences, Nankai University, Tianjin 300071, China

ARTICLE INFO

Article history:
Received 15 May 2013
Received in revised form 1 August 2013
Accepted 2 August 2013
Available online 7 August 2013

Keywords:
Carboxymethyl chitosan
Poly (amidoamine) dendrimer
Core–shell nanoparticles
pH-sensitive
Intracellular lysozyme delivery

ABSTRACT

Intracellular delivery of native, active proteins is challenging due to the fragility of most proteins. Herein, a novel polymer/protein polyion complex (PIC) nanoparticle with core–shell structure was prepared. Carboxymethyl chitosan-grafted-terminal carboxyl group-poly(amidoamine) (CM-chitosan-PAMAM) dendrimers were synthesized by amidation and saponification reactions. ^{1}H NMR was used to characterize CM-chitosan-PAMAM dendrimers. The TEM images and results of lysozyme loading efficiency indicated that CM-chitosan-PAMAM dendrimers could self-assemble into core–shell nanoparticles, and lysozyme was efficiently encapsulated inside the core of CM-chitosan-PAMAM dendrimer nanoparticles. Activity of lysozyme was completely inhibited by CM-chitosan-PAMAM Dendrimers at physiological pH, whereas it was released into the medium and exhibited a significant enzymatic activity in an acidic intracellular environment. Moreover, the CM-chitosan-PAMAM dendrimer nanoparticles did not exhibit significant cytotoxicity in the range of concentrations below 3.16 mg/ml. The results indicated that these CM-chitosan-PAMAM dendrimers have excellent properties as highly potent and non-toxic intracellular protein carriers, which would create opportunities for novel applications in protein delivery.

1. Introduction

The development of intracellular protein therapeutics has been hampered by the limitations arising from the nature of proteins. These limitations include structural fragility, and low serum stability (Lu, Yang, & Sega, 2006; Zhao et al., 2011). All these obstacles require suitable protein delivery carriers that can not only protect the protein cargo from denaturation and proteolysis during circulation and endocytosis, but also release the protein cargo in native forms when the desired destination (i.e. the cytosol) is reached (Davis, 2008; Heath & Davis, 2008). In order to address these requirements, nanoscale carriers for intracellular protein delivery have been reported to date, including lipid-based colloidal carriers (Hu, Hong, & Yuan, 2004; Martins, Sarmento, Ferreira, & Souto, 2007; Mehnert & Mäder, 2001; Zelphati et al., 2001), inorganic nanoparticles (Bale et al., 2010; Ghosh et al., 2010; Medintz et al., 2008; Shimkunas et al., 2009; Slowing, Trewyn, & Lin, 2007), nanotubes (Crinelli et al., 2010; Kam, Liu, & Dai, 2006; Kam, Jessop, Wender, & Dai, 2004) and protein-mediated carriers (Abbing et al., 2004; Cronican et al., 2010; Lim, Cho, Lee, Chung, & Chung, 2009). Although many of these carriers have shown improved performance in protein protection and membrane penetration, covalent modification of proteins is usually required, which could disturb protein folding and impair biological activity (Christian et al., 2009; Parveen & Sahoo, 2006). Otherwise, noncovalent carriers may exhibit low delivery efficiency and encounter other difficulties because of colloidal instability (Ayame, Morimoto, & Akiyoshi, 2008).

Nanoscale polyion complex (PIC) generating from the self-assembly of proteins with natural or synthetic polymers has drawn increasing attention especially for application in therapeutic protein delivery (Calvo, Remunan-Lopez, Vila-Jato, & Alonso, 1997; Harada & Kataoka, 1998; Jintapattanakit et al., 2007; Lee et al., 2007). As a non-covalent method, PIC is formed by simply mixing the drug with oppositely charged polymer mediated by electrostatic-attraction interaction. The PIC formation results in an optically homogeneous system with high thermodynamic stability (Ohya et al., 2011). Furthermore, some PIC formations with pH-sensitivity are even facilitating the endosomal escape of protein drugs. Kataoka's group (Lee et al., 2007) previously developed a new approach for intracellular protein delivery using a pH-sensitive polymer containing citraconic amide. In this strategy, the

* Corresponding author. Tel.: +86 22 2740 2893; fax: +86 22 2740 3389.
E-mail addresses: yaofanglian@tju.edu.cn, yaofanglian@gmail.com (F. Yao).

0144-8617/$ – see front matter © 2013 Elsevier Ltd. All rights reserved.
http://dx.doi.org/10.1016/j.carbpol.2013.08.005

protein drugs were encapsulated by the pH-sensitive polymer via electronic interaction. They exploited pH-dependent degradation mechanism that allows disintegration of PIC formation and release of the cargo. Despite this pH-dependent disintegration strategy, a simple yet effective pH-responsive expansion strategy is also desirable.

In this study, the CM-chitosan-PAMAM dendrimers were synthesized by grafting terminal ester group-PAMAMs onto carboxylmethyl chitosan (CM-chitosan) chains and then the ester groups were converted into carboxyl groups, and both the structure and the size of CM-chitosan-PAMAM dendrimer nanoparticles were adjusted through choosing to use different generation PAMAM dendrimers and controlling the substitution degree of CM-chitosan-PAMAM dendrimer. The pH-sensitivity and cytotoxicity of CM-chitosan-PAMAM dendrimers were characterized. With the CM-chitosan-PAMAM dendrimers, we also developed a novel nanocarrier that can promptly release its protein cargo intracellularly by generating a repulsive electrostatic force owing to the charge conversion of the carrier at the endosomal pH (5.1).

2. Experimental

2.1. Materials

Carboxymethyl chitosan (CM-chitosan) with a degree of deacetylation of 85% and degree of substitution of 83% was purchased from Zhejiang Aoxing Biotechnology Co., Ltd. Methyl acrylate (MA) and ethylenediamine (EDA) were redistilled just before use. Lysozyme was obtained from Bio Basic Inc. Ultrapure water was obtained from an ultrapure-water purification system. All other chemicals purchased were analytically pure and used without further purification.

2.2. Synthesis of PAMAM dendrimers

The preparation of PAMAM dendrimers of each generation was achieved by the repetition of two processes: (1) Michael addition of MA to amino groups as initiator core and (2) terminal amidation of the resulting ester moieties with alkylene diamine (Tomalia et al., 1985).

The Michael addition step was conducted as follows: EDA (7.92 g, 0.132 mol) was blended with MA (91.2 g, 1.06 mol) at 0 °C under vigorous agitation for 10 min. Methanol (125 ml) was added dropwise to the mixture. The mixture temperature was then allowed to rise to 35 °C and the mixture was stirred for 21 h. The solvent and excess MA were subsequently removed under reduced pressure at 50 °C and the 0.5GPAMAM-ester (terminal ester group-hyperbranched 0.5GPAMAM) was left.

The amidation step was carried out as follows: EDA (81 g, 1.35 mol) was carefully added to a vigorously stirred solution of 0.5GPAMAM-ester (15 g, 0.037 mol) in methanol (225 ml) at 0 °C to keep the mixture at room temperature. Then, the mixture was stirred for 72 h at room temperature. The solvent and excess EDA were removed under reduced pressure at a temperature not higher than 72 °C to yield the 1.0GPAMAM-NH_2 (terminal amino group-hyperbranched 1.0GPAMAM).

The second round synthesis was then repeated as above, except that concentration of MA is two times higher and concentration of EDA is three times higher than that in the first round synthesis, to yield the 1.5GPAMAM-ester and 2.0GPAMAM-NH_2 products, and then again to yield the 2.5GPAMAM-ester product. The yield of 0.5GPAMAM-ester, 1.5GPAMAM-ester and 2.5GPAMAM-ester was 99.6%, 95.6% and 93.59% respectively.

2.3. Preparation of CM-chitosan-PAMAM dendrimer nanoparticles

The modification of carboxymethyl chitosan with varying amounts of hyperbranched PAMAM-ester was carried out as follows: CM-chitosan (200 mg) and 0.5GPAMAM-ester (at different molar ratios of PAMAM to NH_2 in CM-chitosan of 1/5, 1/10, 1/15, 1/20, 1/25 and 1/30 respectively) were dissolved in ultrapure water (50 ml). The mixture was stirred in 35 °C for 3 days, followed by dialyzing for 3 days, and lyophilizing to obtain CM-chitosan-PAMAM-ester. The saponification of the terminal ester groups of CM-chitosan-PAMAM-ester to carboxyl groups was conducted as follows: CM-chitosan-PAMAM-ester was suspended in 0.1 M NaOH (20 ml) in room temperature for 1 h. After the reaction, the mixture was dialyzed for 3 days and lyophilized to obtain CM-chitosan-0.5GPAMAM (carboxymethyl chitosan-grafted-terminal carboxyl group-0.5G poly(amidoamine)) dendrimers. The CM-chitosan-1.5GPAMAM (carboxymethyl chitosan-grafted-terminal carboxyl group-1.5G poly(amidoamine)) and CM-chitosan-2.5GPAMAM (carboxymethyl chitosan-grafted-terminal carboxyl group-2.5G poly(amidoamine)) dendrimer were synthesized as the same approach.

2.4. Characterization of CM-chitosan-PAMAM dendrimer nanoparticles

^{1}H NMR (400 MHz) spectra were recorded on Bruker Avance III 400M spectrometer (Switzerland). Test samples of CM-chitosan and CM-chitosan-PAMAM were dissolved in D_2O prior to ^{1}H NMR measurement. The particle size in phosphate buffered solution (PBS) (10 mM, pH 7.4) was performed using a Zetasizer (3000HS, Malvern Instruments, England) by dynamic light scattering technique. The morphology of CM-chitosan-PAMAM dendrimer nanoparticles was observed by a transmission electron microscope (TEM, JEM100CXII, Japan).

2.5. Preparation and characterization of polymer/protein PIC nanoparticles

CM-chitosan/lysozyme and CM-chitosan-PAMAM/lysozyme PIC nanoparticles were prepared at different polymer/protein weight ratios by adding CM-chitosan or CM-chitosan-PAMAM to a phosphate buffered solution (PBS) (10 mM, pH 7.4) of lysozyme (1 mg/ml), followed by vortexing for 5 s and incubating at room temperature for 3 h. Zeta-potential of the nanoparticles was determined by a Zetasizer (3000HS, Malvern Instruments, England) by dynamic light scattering technique. The morphology and size of polymer/protein PIC nanoparticles were further analyzed using a transmission electron microscope (TEM, JEM100CXII, Japan). XRD for polymer/protein PIC was measured using a BDX-3300 diffractometer (Rigaku D/max 2500 v/pc) with CuKα radiation under the operating conditions of 40 kV and 200 mA, and goniometer angular increment of 8 °/min.

2.6. Lysozyme condensation and loading efficiency

To estimate the lysozyme loading efficiency at neutral pH, polymer/protein PIC nanoparticle solutions were prepared at different polymer/protein weight ratios ranging from 0.4/1 to 2.0/1. The mixture was centrifuged at 14,000 rpm for 30 min at 4 °C. Aliquots of the supernatant were collected and the protein content was determined using a standard Coomassie Blue assay (Bezemer et al., 2000). Indirectly, the loading efficiency was determined by measuring the difference between the total amount of lysozyme added to the solution and the amount of free lysozyme left in the supernatant.

2.7. Investigation of lysozyme release from polymer/protein PIC nanoparticles at physiological pH and endosomal pH

The expansion of CM-chitosan-PAMAM dendrimer nanoparticles with the pH decrease from 7.4 (physiological pH) to 5.1 (endosomal pH) was investigated by DLS measurements. The nanoparticle solutions were titrated from pH 7.4 to pH 5.1 by regular addition of small aliquots of 0.25 M HCl solution using an MTP-2 multipurpose titrator (Malvern Instruments, Malvern). Simultaneously, particle size was determined at an interval of half-unit of pH.

In order to investigate the protein release behavior response to endosomal acidification (pH value decreases from 7.4 (physiological pH) to 5.1 (endosomal pH)), the polymer/protein (prepared in PBS at the weight ratio of 1.6/1) PIC nanoparticle solutions were acidized to pH 5.1 with 1 M HCl solution and incubated for 30 min. The lysozyme activity released from the polymer/protein PIC nanoparticles before and after the acidification was evaluated respectively using a well-known method using the Micrococcus luteus cell suspension described by Harada (Harada & Kataoka, 1999). Briefly, after 150 μl of the sample solution was mixed with 30 μl of ML cell stock solution, the transmittance at 450 nm was measured immediately at 37 °C. The absorbance variation for the first 1 min was used for the calculation of the relative activity. The relative activity is calculated from the following equation.:

$$\text{Activity}(\%) = \Delta A(\text{sample solution})/\Delta A_0(\text{control solution})$$

The control solution is free lysozyme solution, and it was prepared with the same amount of lysozyme as that in the PIC nanoparticle solutions.

2.8. Cytotoxicity in vitro of CM-chitosan-PAMAM dendrimers

L929 mouse fibroblast cells (100 μl, 8×10^4 cells/ml) in DMEM containing 10% fetal calf serum (FCS) were seeded into a 96-well plate and cultured in a humidified atmosphere containing 5% CO_2 at 37 °C. After preincubation for 18 h, the media were removed and cells were mixed with solutions of CM-chitosan and CM-chitosan-PAMAM (PBS, pH 7.4) at different concentrations which were sterilized by UV irradiation overnight prior to use. After 24 h of incubation, the samples were replaced by 100 μl of MTT (0.5 mg/ml in HBSS, pH 7.4) solution, and the cells were incubated for further 3 h at 37 °C. The test solutions were decanted, followed by the addition of 150 μl of DMSO to solubilize formed formazan crystals. The cells cultured without exposure to the sample solutions were used as controls. The optical density at 490 nm of the resultant solutions was measured using a microplate reader (Molecular Devices Corporation, Palo Alto, CA, USA). The cell viability was expressed as the percentage of A_{490} of the sample to the control. All of the above tests were carried out in triplicate and the data were expressed as means ± standard deviation (SD).

3. Results and discussion

3.1. Preparation and characterization of CM-chitosan-PAMAM dendrimers

Three different CM-chitosan-PAMAM dendrimers were synthesized by amidation and saponification reactions. The reason for choosing low generation PAMAM-ester (0.5G, 1.5G and 2.5G) is that high generation PAMAM can induce cytotoxic effects (Lee, MacKay, Fréchet, & Szoka, 2005). During the amidation reactions, crosslinking reactions may occur because of the abundant bonding sites in PAMAM-ester. In order to prevent or minimize the crosslinking reactions, a series of CM-chitosan-PAMAM

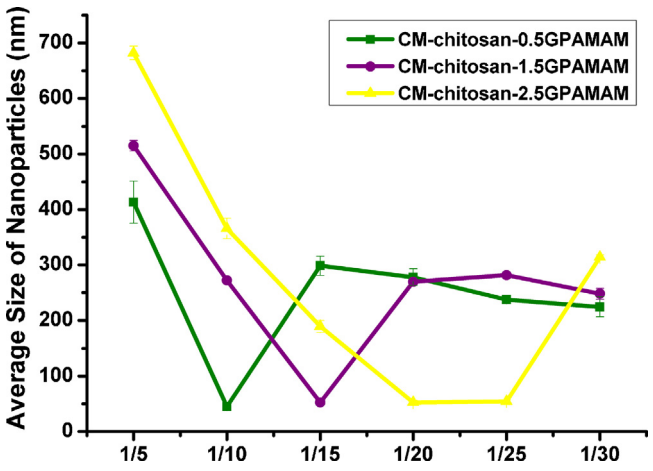

Fig. 1. Size distributions of three kinds of CM-chitosan-PAMAM dendrimer nanoparticles prepared at different molar ratios of PAMAM to NH_2 in CM-chitosan in PBS at 25 °C measured by DLS.

dendrimer nanoparticles were synthesized at different molar ratios of PAMAM-ester to CM-chitosan. As shown in Fig. 1, in terms of CM-chitosan-1.5GPAMAM, in the range of the feeding ratio (the molar ratio of PAMAM-ester to NH_2 in CM-chitosan) upon or below 1/15, the size of the resultant nanoparticles is larger than 200 nm, whereas 30–60 nm under the condition that the CM-chitosan-1.5GPAMAM synthesized at the feeding ratio of 1/15.

In the range of the feeding ratio below 1/15, only a few PAMAMs are grafted onto the CM-chitosan. The CM-chitosan-PAMAM dendrimer with such a low grafting degree is supposed to possess a similar physical and chemical property with CM-chitosan. It should be also noted that the inter or intra molecular hydrogen bonding between carboxyl and amino groups of the CM-chitosan main chain may occur, and result in the aggregation of the nanoparticles. This deduction was also evidenced by the previous study (Aiping, Jianhong, & Wenhui, 2006) which reported the use of CM-chitosan aggregations for the effective loading and controlled release of camptothecin. Therefore, this kind of nanoparticle aggregations could well explain the big size of CM-chitosan-PAMAM dendrimer synthesized at lower feeding ratio (Fig. S1, supplementary data).

With the growth of amount of PAMAM-ester grafted onto CM-chitosan, the grafted PAMAM could generate enough driving force including hydrogen bond and hydrophobic interaction, to form CM-chitosan-PAMAM dendrimer core–shell nanoparticles with appropriate size (about 50 nm). However, as shown in Fig. 1, in the range of feeding ratios upon 1/15, sizes of the resultant CM-chitosan-1.5GPAMAM nanoparticles are more than 200 nm. It could be explained that the presence of the excess PAMAM-ester may induce a serious crosslinking among separate CM-chitosan-PAMAM dendrimer nanoparticles with appropriate size (Fig. S1, supplementary data).

Vonarbourg et al. (Vonarbourg, Passirani, Saulnier, & Benoit, 2006; Vonarbourg, Passirani, Saulnier, Benoit, et al., 2006) have proved that the architecture of nanoparticles strongly dictates the opsonin adsorption, and consequently the phagocytosis. Furthermore, their studies also have demonstrated that the consumption of the complement increases with the size of the nanoparticles and it is more difficult to achieve the proper geometric configuration for efficient complement activation on the most curved surface of the smallest particles than the larger ones. In order to avoid the nanoparticles being engulfed through the phagocytosis pathway, nanoparticle with appropriate size is desired. It also have been recently demonstrated that the optimal cellular uptake of particles by endocytosis occurs with particles that have diameters about 50 nm (Gao, Shi, & Freund, 2005). Therefore the optimized

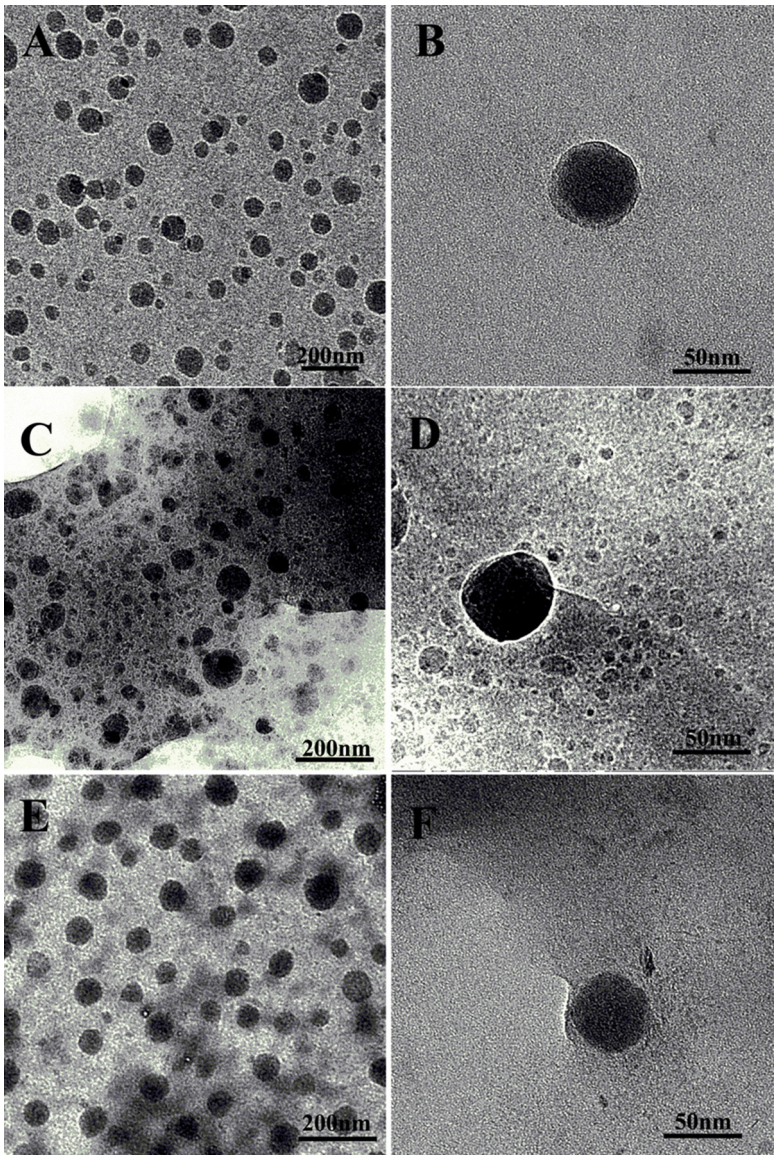

Fig. 2. TEM images of CM-chitosan-0.5GPAMAM dendrimer nanoparticles with (A) low-magnification and (B) high-magnification, CM-chitosan/lysozyme PIC nanoparticles with (C) low-magnification and (D) high-magnification, CM-chitosan-0.5GPAMAM/lysozyme PIC nanoparticles with (E) low-magnification and (F) high-magnification.

feeding ratios for synthesis of CM-chitosan-PAMAM dendrimer nanoparticles with appropriate size are found to be 1/10, 1/15, 1/25 for CM-chitosan-0.5GPAMAM, CM-chitosan-1.5GPAMAM and CM-chitosan-2.5G PAMAM respectively. (The synthesis results of CM-chitosan-PAMAM dendrimers synthesized at optimized feeding ratios are shown in Table S1 in supplementary data). It should be noted that all the CM-chitosan-PAMAM dendrimers used in the following tests and experiments were synthesized at the optimized feeding ratios.

Fig. S2 in supplementary shows the ^{1}H NMR spectra of CM-chitosan and three different CM-chitosan-PAMAM dendrimers. Comparing with the ^{1}H NMR spectrum of CM-chitosan, the presence of the new peak at around 2.8 ppm in the spectra of CM-chitosan-PAMAM dendrimers presumably were caused by the methylene protons from carboxyl terminated-PAMAMs, as a result of the chemical bonding between ester terminated-PAMAMs and CM-chitosan (Peterson, Allikmaa, Subbi, Pehk & Lopp, 2003). The degree of substitution (DS) of CM-chitosan-PAMAM dendrimers could be estimated by the signal at 2.4 ppm against that of $NHCOCH_3$ and the results were shown in Table S1 in supplementary data.

3.2. Self-assembling of CM-chitosan-PAMAM dendrimers in aqueous solution

CM-chitosan-PAMAM dendrimers are proposed to form nanoparticles with PAMAM cores and CM-chitosan shells in aqueous solution via self-assembly, driven by the combination of hydrophobic interaction and hydrogen bonding among PAMAMs. The plentiful free carboxyl groups of PAMAM that are not dissociated at physiological pH contribute to the formation of strong hydrogen bonds among each other, and PAMAMs serve as the hydrophobic core. A similar nanoparticle formation mechanism of CM-HTCC/PAMAM-NH_2 has been demonstrated by our previous study (Wen et al., 2012).

TEM characterization (Fig. 2(A)) clearly demonstrates that the synthesized CM-chitosan-PAMAM dendrimers consistently exhibit as nanoparticles with sphere-like shapes and average diameters of

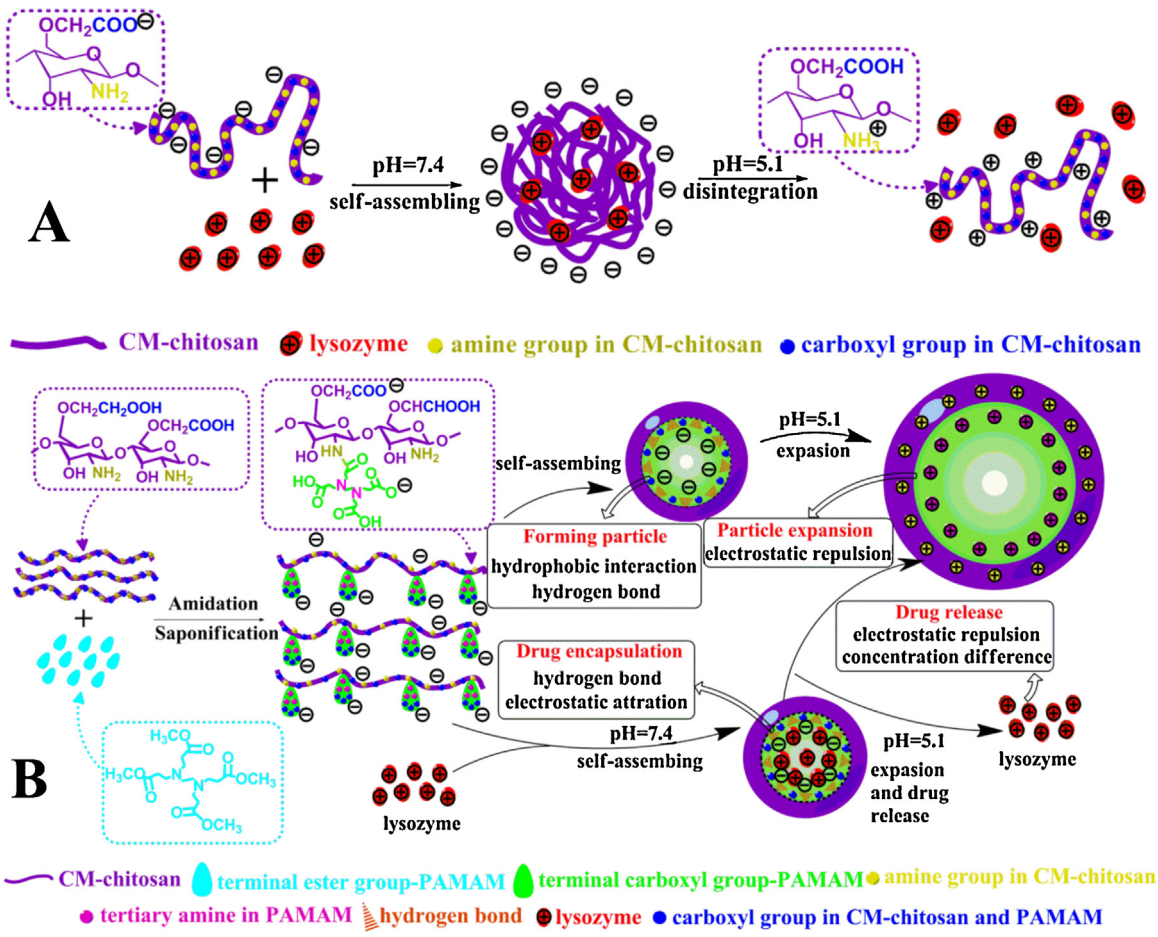

Fig. 3. (A) Schematic representation of the encapsulation and release mechanism of lysozyme from CM-chitosan/lysozyme PIC nanoparticles. (B) Schematic representation of synthesis and self-assembling for CM-chitosan-PAMAM dendrimer nanoparticles, and the encapsulation and release mechanism of lysozyme from CM-chitosan-PAMAM/lysozyme PIC nanoparticles.

30–60 nm and the detailed structure of the nanoparticles could be observed from Fig. 2(B).

3.3. *Protein encapsulation by the CM-chitosan-PAMAM dendrimer nanoparticles and CM-chitosan: characterization and loading efficiency*

Lysozyme was selected as a model protein drug to be incorporated by the negatively charged CM-chitosan-PAMAM dendrimer nanoparticles at physiological pH because lysozyme would be positively charged over a wide pH range due to its high isoelectric point (~pH 10.8), and had practical usage in drug delivery applications as lytic enzyme. Detailed physicochemical characteristics available for this protein was another charming advantage facilitating to gain insight into polyion complex (PIC) formation mechanisms of polymers and proteins.

Besides CM-chitosan-PAMAM dendrimers, CM-chitosan was also studied as a control. CM-chitosan itself could not self-assemble into a core–shell nanoparticle. However, the negatively-charged CM-chitosan can form nanoscale PIC gel spheres with cationic proteins, as represented in Fig. 3(A).

The primary requirement for polymers to function as intracellular delivery carriers is the desiring ability to condense their content into nanoscale particles. It is expected that the PAMAM in the core of the CM-chitosan-PAMAM dendrimer nanoparticles may form hydrogen bond with lysozyme. Moreover, the CM-chitosan-PAMAM dendrimers are regarded as polyanions at physiological pH (7.4), because of partial dissociation of the carboxyl groups in CM-chitosan and PAMAM. Lysozyme, as an enzyme with an isoelectric point of 10.8, will display positive charges under these conditions. Charge interactions between CM-chitosan-PAMAM dendrimer nanoparticles and lysozyme could be anticipated and would probably endow them with the capacity to appear as the polyion complex (PIC) nanoparticles with a core–shell structure (Fig. 3(B)).

Fig. 4 shows that the zeta potential of the polymer/protein PIC nanoparticles decreases significantly with the growth of polymer weight percentage in the polyion complexes, implying that CM-chitosan-PAMAM dendrimers or CM-chitosan have a greater effect on the zeta potential of the polymer/protein PIC nanoparticles than lysozyme. Lysozyme with molecular weight of 14,300 has 11 arginine and six lysine residues, and the positive charge density resulting from arginine or lysine is one residue per 841 Da. The negative charge density resulting from carboxyl group of CM-chitosan and CM-chitosan-PAMAM dendrimers are calculated similarly and the corresponding results are approximately one per 260 Da and 230 Da respectively, which are remarkably higher than arginine or lysine density in lysozyme. As a result, the higher density of negative charge groups in CM-chitosan-PAMAM dendrimers or CM-chitosan would play a more important role on the zeta potential of the polymer/protein PIC nanoparticles as compared to the positive charge groups of lysozyme. In addition, at 60% weight percentage of polymers in polymer/protein PIC nanoparticles, the zeta potential of polymer/protein PIC nanoparticles nearly is equal to

Table 1
Lysozyme loading efficiencies of polymer/protein PIC nanoparticles prepared at different polymer/protein weight ratios in PBS (pH 7.4)[a].

Polymer/protein weight ratio	Lysozyme loading efficiency (%)			
	CM-chitosan	CM-chitosan-0.5GPAMAM	CM-chitosan-1.5GPAMAM	CM-chitosan-2.5GPAMAM
0.4/1	71.68 ± 0.62	87.03 ± 0.46	86.52 ± 0.55	84.42 ± 0.75
0.8/1	72.58 ± 0.83	88.08 ± 0.28	87.14 ± 0.42	86.75 ± 0.43
1.2/1	73.52 ± 0.28	89.40 ± 0.33	87.50 ± 0.68	88.87 ± 0.54
1.6/1	74.65 ± 0.48	90.46 ± 0.57	89.85 ± 0.27	90.18 ± 0.73
2.0/1	76.23 ± 0.39	91.08 ± 0.34	90.51 ± 0.35	90.50 ± 0.38

[a] The reported values were determined by measuring the difference of the amount of lysozyme between the initial addition and residue in the supernatant. The initial lysozyme concentration is 1 mg/ml.

the pure polymers zeta potential (corresponding to the data at 100% weight percentage of polymers in polymer/protein PIC nanoparticles as shown in Fig. 4), indicating almost all the lysozymes are condensed by the polymer. It should be mentioned that the data at 0% weight percentage of polymers in polymer/protein PIC nanoparticles stand for the zeta potential of pure lysozyme.

Table 1 gives the lysozyme loading efficiencies of the polymer/protein PIC nanoparticles in phosphate buffer solution (10 mM, pH 7.4) using a standard Coomassie Blue assay.

It can be seen that the lysozyme loading efficiency of CM-chitosan/lysozyme PIC nanoparticles is relatively low, as compared to the CM-chitosan-PAMAM/lysozyme PIC nanoparticles. This noticeable difference in lysozyme loading efficiency between CM-chitosan and CM-chitosan-PAMAM dendrimers might be primarily attributed to the structure of the polymers. CM-chitosan-PAMAM dendrimers exist as core–shell nanoparticles, and the PAMAM core serves as a big cavity to incorporate the enzyme, whereas CM-chitosan in the form of polyanions encapsulates oppositely charged lysozyme by forming a simple gel sphere via electrostatic interaction. Furthermore, higher negative charge density of CM-chitosan-PAMAM dendrimers caused by the partial dissociation of the carboxyl groups in PAMAM core presumably contributes to more effective encapsulation of lysozyme compared to CM-chitosan. Additionally, a large amount of secondary amine and undissociated carboxyl groups in PAMAM core will also associate with lysozyme through the formation of hydrogen bond. Because the lysozyme loading efficiency is almost the highest as the PIC nanoparticles were prepared at polymer/protein weight ratio of 1.6/1 for the three different kinds of CM-chitosan-PAMAM dendrimer, all the polymer/protein PIC nanoparticles used in the following experiments are prepared at the weight ratio of 1.6/1.

The above lysozyme loading experiment permits to estimate the quantity of the lysozyme encapsulated in polymer/protein PIC nanoparticles. Additionally, the diffraction spectra of polymer/protein PIC nanoparticles (Fig. S3, supplementary data) could provide the information about the ability of polymer/protein PIC nanoparticles to keep activity of lysozymes. The strong crystalline peaks at $2\theta = 32.1^\circ$ and 45.8°, attributed to the relatively crystal lattice of lyszoyme (Katrusiak & Dauter, 1996), are observed. And it has been verified that lysozyme retains its activity within the constraints of crystal lattice by various studies (Jolles, 1996). These results indicate that activity of lysozyme is not destroyed as encapsulated by CM-chitosan and CM-chitosan-PAMAM.

TEM microscopy (Fig. 2(C–F)) visualizes a well-shaped spherical structure of the polymer/protein PIC nanoparticles. The particle sizes of separate polymer/protein PIC nanoparticles are about 50 nm and the size distribution is narrow. Moreover, plenty of free lysozyme particles, whose size is less than 10 nm are observed clearly in Fig. 2(C and D) for CM-chitosan/lysozyme rather than the case as Fig. 2(E and F) for CM-chitosan-PAMAM/lysozyme PIC nanoparticles. These results indicate that CM-chitosan-PAMAM dendrimer nanoparticles could encapsulate lysozyme more effectively than CM-chitosan, which is in accordance with the results of lysozyme loading efficiency.

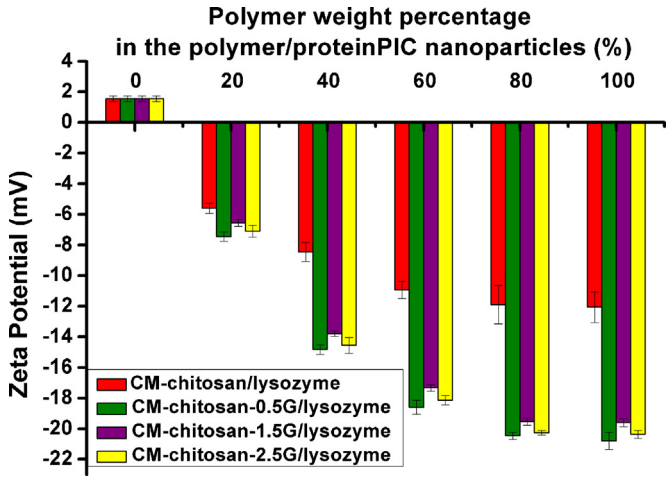

Fig. 4. Zeta-potentials of polymer/protein PIC nanoparticles measured as a function of the polymer weight percentage in the polymer/protein PIC nanoparticles by DLS at 25 °C.

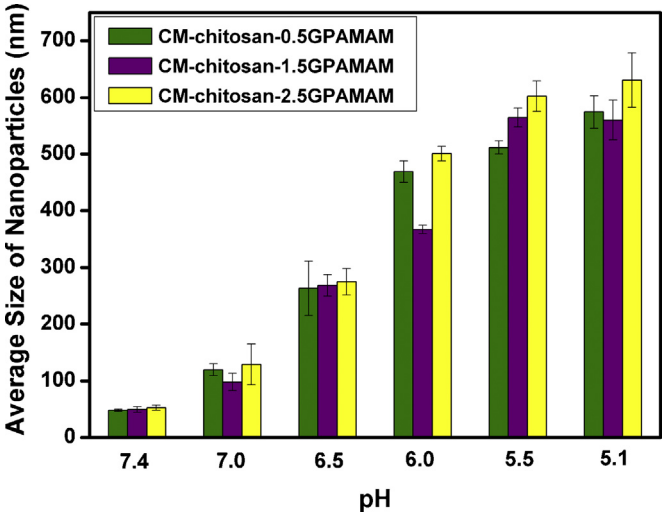

Fig. 5. Size changing of CM-chitosan-PAMAM dendrimer nanoparticles during pH titration from pH 7.4 to 5.1, representing the pH of the physiological and endosomal environments respectively.

Table 2
Lysozyme activity released from polymer/protein PIC at pH 7.4 and 5.1, representing the pH of the physiological and endosomal environments respectively [a].

pH	Lysozyme activity (%)			
	CM-chitosan	CM-chitosan-0.5GPAMAM	CM-chitosan-1.5GPAMAM	CM-chitosan-2.5GPAMAM
7.4	7.26 ± 0.34	3.40 ± 0.32	5.15 ± 0.48	5.48 ± 0.44
5.1	41.67 ± 1.09	52.38 ± 0.41	63.81 ± 1.09	68.81 ± 0.41

[a] The relative activity is expressed as a percentage of the free lysozyme activity.

3.4. Release of lysozyme from polymer/protein PIC nanoparticles at endosomal pH.

Another requirement for polymers to function as intracellular delivery carriers is that the carrier must be capable to efficiently unpack the therapeutic payload once the delivery system is internalized by the cell (Pack, Hoffman, Pun, & Stayton, 2005; Schaffer, Fidelman, Dan, & Lauffenburger, 2000). Herein the expansion of CM-chitosan-PAMAM dendrimer nanoparticles with a core–shell structure in the intracellular environment was illustrated by their size change as the drop of pH by DSL measurenents (Fig. 5).

As shown in Fig. 5, the average size of CM-chitosan-PAMAM dendrimer nanoparticles significantly increases from about 50 nm to more than 600 nm when the pH decreases from 7.4 (physiological pH) to 5.1 (endosomal pH). Since CM-chitosan-PAMAM dendrimers could be regarded as ampholyte due to the presence of carboxyl groups and amino groups, the decrease in pH occurring during endosomal acidification is supposed to influence the structure and size of the nanoparticles. Primarily, the protonation of amino groups in CM-chitosans and tertiary amines in PAMAMs will lead to a strong electrostatic repulsion in CM-chitosan-PAMAM dendrimer nanoparticles. Moreover, the CM-chitosan-PAMAM dendrimer would also swell as a result of the protonation and hydration of its amino groups and tertiary amines. Therefore increase of particle size upon decreasing pH might be explained by the CM-chitosan-PAMAM dendrimers undergoing a conformational change caused by the charge conversion and the hydration during the endosomal acidification. Thus, the strategy proposed herein is that the pH-sensitivity of the CM-chitosan-PAMAM dendrimer nanoparticles would be applied to the drug delivery field requiring selective controlled release, for example, the specific release at endosomal pH.

Table 2 gives the lysozyme activity released at pH 7.4 and 5.1 representing for the physiological pH and endosomal pH respectively. The lysozyme activity at pH 7.4 (physiological pH) was investigated to illustrate the inhibition ability of polymers to the lysozyme activity by the encapsulation and preserve the enzyme inside the core of the nanoparticles. The lysozyme activity at pH 5.1 (endosomal pH) was carried out to evaluate the ability of polymers to recover the lysozyme activity after lysozyme released from the nanoparticles caused by endosomal acidification. The lysozyme activity was measured by a well-known method using the Micrococus luteus cell suspension. Considering the pH-dependence of protein activity, the free lysozyme activity at pH 7.4 and 5.1 was both investigated respectively.

As shown in Table 2, the lysozyme activity is almost completely suppressed in polymer/protein PIC nanoparticles at pH 7.4, it would be possible that the encapsulation of lysozyme by polymer/protein PIC nanoparticles could prevent the enzyme to display its activity in an extracellular environment. However, after the pH drops to endosomal pH (5.1), recoveries of enzymatic activity are observed for both CM-chitosan/lysozyme and CM-chitosan-PAMMA/lysozyme PIC nanoparticles, indicating that the activity of lysozyme are not damaged after interacting with CM-chitosan and CM-chitosan-PAMAM. The good compatibility between chitosan-based materials and lysozyme could also be proved by a previous study (Muzzarelli, Barontini, & Rochetti, 1978), which reported that lysozyme retained its activity to some extent after interacting with the chitosan columns. Additionally, it could be observed that the recovery of enzymatic activity is higher for CM-chitosan-PAMAM/lysozyme PIC nanoparticles than that for CM-chitosan/lysozyme PIC nanoparticles lacking the core–shell structure in Table 2. It may be suggested that although the CM-chitosan/lysozyme PIC nanoparticles have been disintegrated at endosomal pH, there is still a weak interaction between lysozyme and CM-chitosan due to the mechanism of nanoparticle formation. Because the direct contact of lysozyme with bacterial cell wall is required for a full activity, the bounding of lysozyme to CM-chitosan chains, even though very weak, can reduce the lysozyme activity. Nevertheless, CM-chitosan-PAMAM/lysozyme PIC nanoparticles can selectively expand with the pH and then lysozyme is released totally out of CM-chitosan-PAMAM/lysozyme PIC nanoparticles, maintaining its higher enzymatic activity at the same time.

Table 2 also shows that more lysozyme with enzymatic activity was released from the CM-chitosan-PAMAM dendrimer synthesized by higher generation PAMAM and CM-chitosan (CM-chitosan-higher generation PAMAM dendrimer). Presumably, this result correlated with that the protonation of more tertiary amino groups existing in the core of CM-chitosan-higher generation PAMAM dendrimer nanoparticles during the pH decrease from physiological pH to endosomal pH. Therefore, stronger electrostatic repulsion was generated between the protonated tertiary amine and cationic lysozyme, and more lysozyme was released consequently. It worth noting that this pH-responsive off–on switching of the enzymatic activity in these nanoparticles is a promising property for minimizing off-target effects in targeting delivery.

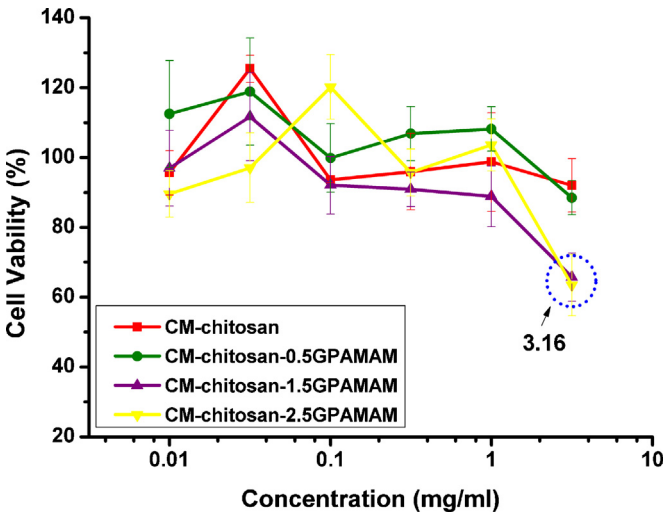

Fig. 6. Viability of L929 fibroblast cells after incubation with polymers at different concentrations, determined by MTT assay.

3.5. Cytotoxicity in vitro

An L929 fibroblast cell line was exposed to CM-chitosan-PAMAM dendrimers solutions at different concentrations over a period of 24 h and cell viability was investigated by a MTT test.

As shown in Fig. 6, CM-chitosan-PAMAM dendrimers do not induce any toxicity in the range of concentration below 3.16 mg/ml. The viability of L929 cells slightly decreased in the presence of CM-chitosan-1.5GPAMAM or CM-chitosan-2.5GPAMAM dendrimer at a concentration of 3.16 mg/ml after 24 h, which indicates moderate cytotoxic effects. The concentration-dependence of the cytotoxicity of CM-chitosan-PAMAM dendrimers is in agreement with previous study that the biocompatibility of polymers may be affected by the concentration in a certain extent. Additionally, the specific reason of good biocompatibility of CM-chitosan-PAMAM dendrimers will be investigated in our future work.

4. Conclusion

Novel nanoparticles with well-controllable structure that consist of a PAMAM dendrimer core and CM-chitosan shell were prepared. These nanoparticles could be able to condense lysozyme and inhibit its activity at physiological pH (7.4). After endosomal acidification (5.1), CM-chitosan-PAMAM dendrimer nanoparticles underwent a charge-converting and tended to expand as evidenced by the increasing particle size. Furthermore, the release of protein cargo remaining a high enzymatic activity from the CM-chitosan-PAMAM/lysozyme PIC nanaoparticles was observed in the mimic endosomal environment. In vitro tests showed that CM-chitosan-PAMAM dendrimer nanoparticles did not exert any significant cytotoxic effect on L929 fibroblasts at concentrations below 3.16 mg/ml. Thus, the novel CM-chitosan-PAMAM core–shell nanoparticles have a great potential to apply for intracellular delivery of protein drugs and genes.

Acknowledgment

This work is supported by National Nature Science Foundation of China 51073119 and 31271016.

Appendix A. Supplementary data

Supplementary data associated with this article can be found, in the online version, at http://dx.doi.org/10.1016/j.carbpol.2013.08.005.

References

Abbing, A., Blaschke, U. K., Grein, S., Kretschmar, M., Stark, C. M., Thies, M. J., et al. (2004). Efficient intracellular delivery of a protein and a low molecular weight substance via recombinant polyomavirus-like particles. *Journal of Biological Chemistry*, *279*(26), 27410–27421.

Aiping, Z., Jianhong, L., & Wenhui, Y. (2006). Effective loading and controlled release of camptothecin by *O*-carboxymethylchitosan aggregates. *Carbohydrate Polymers*, *63*(1), 89–96.

Ayame, H., Morimoto, N., & Akiyoshi, K. (2008). Self-assembled cationic nanogels for intracellular protein delivery. *Bioconjugate Chemistry*, *19*(4), 882–890.

Bale, S. S., Kwon, S. J., Shah, D. A., Banerjee, A., Dordick, J. S., & Kane, R. S. (2010). Nanoparticle-mediated cytoplasmic delivery of proteins to target cellular machinery. *ACS Nano*, *4*(3), 1493–1500.

Bezemer, J., Radersma, R., Grijpma, D., Dijkstra, P., Feijen, J., & Van Blitterswijk, C. (2000). Zero-order release of lysozyme from poly (ethylene glycol)/poly (butylene terephthalate) matrices. *Journal of Controlled Release*, *64*(1), 179–192.

Calvo, P., Remunan-Lopez, C., Vila-Jato, J., & Alonso, M. (1997). Novel hydrophilic chitosan-polyethylene oxide nanoparticles as protein carriers. *Journal of Applied Polymer Science*, *63*(1), 125–132.

Christian, D. A., Cai, S., Bowen, D. M., Kim, Y., Pajerowski, J. D., & Discher, D. E. (2009). Polymersome carriers: From self-assembly to siRNA and protein therapeutics. *European Journal of Pharmaceutics and Biopharmaceutics*, *71*(3), 463–474.

Crinelli, R., Carloni, E., Menotta, M., Giacomini, E., Bianchi, M., Ambrosi, G., et al. (2010). Oxidized ultrashort nanotubes as carbon scaffolds for the construction of cell-penetrating NF-κB decoy molecules. *ACS Nano*, *4*(5), 2791–2803.

Cronican, J. J., Thompson, D. B., Beier, K. T., McNaughton, B. R., Cepko, C. L., & Liu, D. R. (2010). Potent delivery of functional proteins into mammalian cells in vitro and in vivo using a supercharged protein. *ACS Chemical Biology*, *5*(8), 747–752.

Davis, M. E. (2008). Nanoparticle therapeutics: An emerging treatment modality for cancer. *Nature Reviews Drug Discovery*, *7*(9), 771–782.

Gao, H., Shi, W., & Freund, L. B. (2005). Mechanics of receptor-mediated endocytosis. *Proceedings of the National Academy of Sciences of the United States of America*, *102*(27), 9469–9474.

Ghosh, P., Yang, X., Arvizo, R., Zhu, Z.-J., Agasti, S. S., Mo, Z., et al. (2010). Intracellular delivery of a membrane-impermeable enzyme in active form using functionalized gold nanoparticles. *Journal of The American Chemical Society*, *132*(8), 2642–2645.

Harada, A., & Kataoka, K. (1998). Novel polyion complex micelles entrapping enzyme molecules in the core: Preparation of narrowly-distributed micelles from lysozyme and poly (ethylene glycol)-poly (aspartic acid) block copolymer in aqueous medium. *Macromolecules*, *31*(2), 288–294.

Harada, A., & Kataoka, K. (1999). On–off control of enzymatic activity synchronizing with reversible formation of supramolecular assembly from enzyme and charged block copolymers. *Journal of The American Chemical Society*, *121*(39), 9241–9242.

Heath, J. R., & Davis, M. E. (2008). Nanotechnology and cancer. *Annual Review of Medicine*, *59*, 251–265.

Hu, F., Hong, Y., & Yuan, H. (2004). Preparation and characterization of solid lipid nanoparticles containing peptide. *International Journal of Pharmaceutics*, *273*(1), 29–35.

Jintapattanakit, A., Junyaprasert, V. B., Mao, S., Sitterberg, J., Bakowsky, U., & Kissel, T. (2007). Peroral delivery of insulin using chitosan derivatives: A comparative study of polyelectrolyte nanocomplexes and nanoparticles. *International Journal of Pharmaceutics*, *342*(1), 240–249.

Jolles, P. (1996). *Lysozymes–model enzymes in biochemistry and biology*. Basel; Boston: Birkhauser Verlag.

Kam, N. W. S, Jessop, T. C., Wender, P. A., & Dai, H. (2004). Nanotube molecular transporters: Internalization of carbon nanotube–protein conjugates into mammalian cells. *Journal of The American Chemical Society*, *126*(22), 6850–6851.

Kam, N. W. S., Liu, Z., & Dai, H. (2006). Carbon nanotubes as intracellular transporters for proteins and DNA: An investigation of the uptake mechanism and pathway. *Angewandte Chemie*, *118*(4), 591–595.

Katrusiak, A., & Dauter, Z. (1996). Compressibility of lysozyme protein crystals by X-ray diffraction. *Acta Crystallographica Section D: Biological Crystallography*, *52*(3), 607–608.

Lee, C. C., MacKay, J. A., Fréchet, J. M., & Szoka, F. C. (2005). Designing dendrimers for biological applications. *Nature Biotechnology*, *23*(12), 1517–1526.

Lee, Y., Fukushima, S., Bae, Y., Hiki, S., Ishii, T., & Kataoka, K. (2007). A protein nanocarrier from charge-conversion polymer in response to endosomal pH. *Journal of the American Chemical Society*, *129*(17), 5362–5363.

Lim, Y. T., Cho, M. Y., Lee, J. M., Chung, S. J., & Chung, B. H. (2009). Simultaneous intracellular delivery of targeting antibodies and functional nanoparticles with engineered protein G system. *Biomaterials*, *30*(6), 1197–1204.

Lu, Y., Yang, J., & Sega, E. (2006). Issues related to targeted delivery of proteins and peptides. *The AAPS Journal*, *8*(3), E466–E478.

Martins, S., Sarmento, B., Ferreira, D. C., & Souto, E. B. (2007). Lipid-based colloidal carriers for peptide and protein delivery–liposomes versus lipid nanoparticles. *International Journal of Nanomedicine*, *2*(4), 595.

Medintz, I. L., Pons, T., Delehanty, J. B., Susumu, K., Brunel, F. M., Dawson, P. E., et al. (2008). Intracellular delivery of quantum dot–protein cargos mediated by cell penetrating peptides. *Bioconjugate Chemistry*, *19*(9), 1785–1795.

Mehnert, W., & Mäder, K. (2001). Solid lipid nanoparticles: Production, characterization and applications. *Advanced Drug Delivery Reviews*, *47*(2), 165–196.

Muzzarelli, R. A., Barontini, G., & Rochetti, R. (1978). Isolation of lysozyme on chitosan. *Biotechnology and Bioengineering*, *20*(1), 87–94.

Ohya, Y., Takeda, S., Shibata, Y., Ouchi, T., Kano, A., Iwata, T., et al. (2011). Evaluation of polyanion-coated biodegradable polymeric micelles as drug delivery vehicles. *Journal of Controlled Release*, *155*(1), 104–110.

Pack, D. W., Hoffman, A. S., Pun, S., & Stayton, P. S. (2005). Design and development of polymers for gene delivery. *Nature Reviews Drug Discovery*, *4*(7), 581–593.

Parveen, S., & Sahoo, S. K. (2006). Nanomedicine: Clinical applications of polyethylene glycol conjugated proteins and drugs. *Clinical Pharmacokinetics*, *45*(10), 965–988.

Peterson, J., Allikmaa, V., Subbi, J., Pehk, T., & Lopp, M. (2003). Structural deviations in poly (amidoamine) dendrimers: A MALDI-TOF MS analysis. *European Polymer Journal*, *39*(1), 33–42.

Schaffer, D. V., Fidelman, N. A., Dan, N., & Lauffenburger, D. A. (2000). Vector unpacking as a potential barrier for receptor-mediated polyplex gene delivery. *Biotechnology and Bioengineering*, *67*(5), 598–606.

Shimkunas, R. A., Robinson, E., Lam, R., Lu, S., Xu, X., Zhang, X.-Q., et al. (2009). Nanodiamond–insulin complexes as pH-dependent protein delivery vehicles. *Biomaterials*, *30*(29), 5720–5728.

Slowing, I. I., Trewyn, B. G., & Lin, V. S.-Y. (2007). Mesoporous silica nanoparticles for intracellular delivery of membrane-impermeable proteins. *Journal of The American Chemical Society*, *129*(28), 8845–8849.

Tomalia, D., Baker, H., Dewald, J., Hall, M., Kallos, G., Martin, S., et al. (1985). A new class of polymers: Starburst-dendritic macromolecules. *Polymer Journal*, *17*(1), 117–132.

Vonarbourg, A., Passirani, C., Saulnier, P., & Benoit, J.-P. (2006). Parameters influencing the stealthiness of colloidal drug delivery systems. *Biomaterials*, *27*(24), 4356–4373.

Vonarbourg, A., Passirani, C., Saulnier, P., Simard, P., Leroux, J., & Benoit, J. (2006). Evaluation of pegylated lipid nanocapsules versus complement system activation and macrophage uptake. *Journal of Biomedical Materials Research Part A*, *78*(3), 620–628.

Wen, Y., Tan, Z., Sun, F., Sheng, L., Zhang, X., & Yao, F. (2012). Synthesis and characterization of quaternized carboxymethyl chitosan/poly (amidoamine) dendrimer core–shell nanoparticles. *Materials Science and Engineering: C*, *32*(7), 2026–2036.

Zelphati, O., Wang, Y., Kitada, S., Reed, J. C., Felgner, P. L., & Corbeil, J. (2001). Intracellular delivery of proteins with a new lipid-mediated delivery system. *Journal of Biological Chemistry*, *276*(37), 35103–35110.

Zhao, M., Biswas, A., Hu, B., Joo, K.-I., Wang, P., Gu, Z., et al. (2011). Redox-responsive nanocapsules for intracellular protein delivery. *Biomaterials*, *32*(22), 5223–5230.